Nineteenth International Conference on
Geometry, Integrability and Quantization
June 02–07, 2017, Varna, Bulgaria
Ivaïlo M. Mladenov and
Akira Yoshioka, Editors
**Avangard Prima**, Sofia 2018, pp 168–187
doi: 10.7546/giq-19-2018-168-187


# ON A CLASS OF LINEAR WEINGARTEN SURFACES

VLADIMIR I. PULOV, MARIANA TS. HADZHILAZOVA† and
IVAÏLO M. MLADENOV†

*Department of Physics, Technical University of Varna, Studentska Str. 1, 9010 Varna Bulgaria*

†*Institute of Biophysics and Biomedical Engineering, Bulgarian Academy of Sciences Acad. G. Bonchev Str., Block 21, 1113 Sofia, Bulgaria*

**Abstract.** We consider a class of linear Weingarten surfaces of revolution whose principal curvatures, meridional $k_\mu$ and parallel $k_\pi$, satisfy the relation $k_\mu = (n+1)k_\pi$, $n = 0, 1, 2, \ldots$ . The first two members of this class of surfaces are the sphere $(n = 0)$ and the Mylar balloon $(n = 1)$. Elsewhere the Mylar balloon has been parameterized via the Jacobian and Weierstrassian elliptic functions and elliptic integrals. Here we derive six alternative parameterizations describing the third type of surfaces when $n = 2$. The so obtained explicit formulas are applied for the derivation of the basic geometrical characteristics of this surface.

*MSC*: 53A04, 53A05, 33B15, 33C05, 33E05, 49K10, 49Q10, 49Q20
*Keywords*: Axisymmetric surfaces, elliptic functions, explicit parametrizations, surface geometry, profile curves, Weingarten surfaces, Weierstrassian elliptic functions

CONTENTS

## 1. Introduction

Surfaces whose principal curvatures obey a functional relation are called *Weingarten surfaces*. The surfaces we are interested in belong to the class of *linear Weingarten surfaces of revolution* whose meridional $k_\mu$ and parallel $k_\pi$ principal curvatures satisfy the equation

$$k_\mu = (n+1)k_\pi, \qquad n = 0,\, 1,\, 2,\, \ldots. \tag{1}$$

Hereinafter such surfaces are referred to as *LW*(*n*) *surfaces* or *LW*(*n*) *balloons*. The first two members of this class of surfaces are the sphere $(n \equiv 0)$ and the Mylar balloon $(n \equiv 1)$. The problem of finding the shape of the Mylar balloon was raised by Paulsen [21] in calculus of variations settings: *Find a surface of revolution, enclosing maximum volume, for a given arclength of the directrice.* This variational characterization of the Mylar balloon was generalized later by Mladenov and Oprea [14, 15] for all surfaces *LW*(*n*) associated with arbitrary natural number $n$.
Recently the authors of [23] have introduced another interesting class of the so called constant skew curvature surfaces. In order to give a rigorous formulation behind the equation (1) we assume that the $OZ$-axis is the axis of revolution and the curve, $z = z(x)$, lying in the $XOZ$-plane, is the upper half part of the right hand side of the profile curve of the *LW*(*n*) balloon (Fig. 1). Similarly to the case of the Mylar balloon (cf. [11, 13, 19, 22]) we impose that the curve is smoothly decreasing from its maximum height on the $OZ$-axis to a point on the $OX$-axis, crossing the $OX$-axis at a right angle. In order to meet these requirements we assume that $z(r) = 0$ for some positive $r$, that the derivatives satisfy the conditions $\dot{z}(x) < 0$ for $0 < x < r$, $\dot{z}(0) = 0$ and $\lim_{x\to r} \dot{z}(x) = -\infty$. We demand also that the arclength from $x = 0$ to $x = r$ is fixed to $a$, $a > 0$. It follows from symmetry considerations that the bottom half of the balloon is obtained by reflection of its upper half part through the $XOY$-plane.

The *LW*(*n*) surfaces, defined above, are uniquely characterized as solutions to the following calculus of variations problem [14,15]. *Find the profile curve* (*directrice*) *of a surface of revolution* (*with $OZ$ line taken as an axis of revolution*)

$$z = z(x), \qquad z(r) = 0, \qquad \dot{z}(x) \le 0, \qquad 0 \le x \le r$$

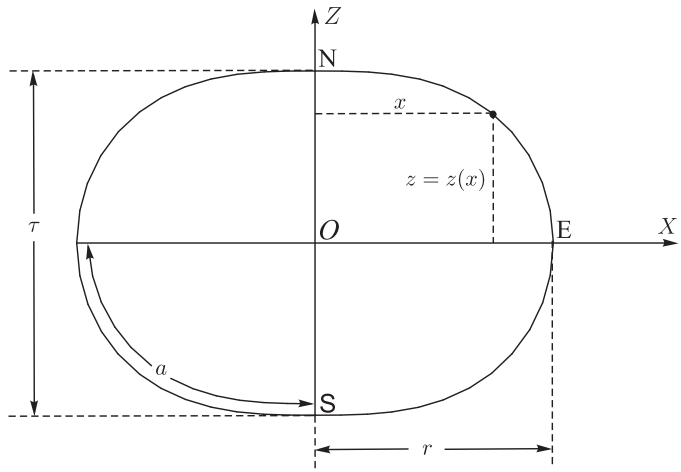


**Figure 1.** A typical profile curve in the $XOZ$-plane of the *LW*($n$) balloon where $a$ is a quarter of the circumference of the profile curve, $r$ is the radius and $\tau$ is the thickness of the balloon.

*by extremizing the $n$-th moment of the function $z(x)$*

$$\mathcal{J}_n[z(x)] = \int_0^r x^n z(x)\mathrm{d}x, \qquad n = 0,\, 1, 2\ldots$$

*subject to the constraint*

$$\int_0^r \sqrt{1+\dot{z}^2(x)}\mathrm{d}x = a, \qquad a > 0$$

*and satisfying the transversality conditions*

$$\dot{z}(0) = 0, \qquad \lim_{x\to r}\dot{z}(x) = -\infty.$$

As it is shown in [15] the respective Euler-Lagrange equation takes the form

$$\frac{\mathrm{d}z}{\mathrm{d}x} = -\frac{x^{n+1}}{\sqrt{r^{2(n+1)} - x^{2(n+1)}}}. \tag{2}$$

The last equation is readily integrated in terms of special functions (for the used special function, cf. [1, 3, 25]). One of the resulting representations [14] of the profile curve of the *LW*(n) balloon is given by the formulas

$$z(x) = \frac{r}{2(n+1)}[B_1(\frac{n+2}{2n+2},\, \frac{1}{2}) - B_{\tau(x)}(\frac{n+2}{2n+2},\, \frac{1}{2})]$$
$$\tau(x) = \left(\frac{x}{r}\right)^{2n+2}, \qquad x \in [0, r], \qquad n = 0,\, 1,\, 2, \ldots \tag{3}$$

where $B_\tau(p, q)$ is the *incomplete beta function* of the real variable $\tau$ and the parameters $p$ and $q$

$$B_\tau(p, q) = \int_0^\tau t^{p-1}(1-t)^{q-1}\mathrm{d}t.$$

By making use of the *Gaussian hypergeometric function* ${}_2F_1(\alpha, \beta; \gamma; \tau)$ in which $\tau \in \mathbb{R}$ is the argument, $\alpha, \beta$ and $\gamma$ are three real parameters and the relation

$$B_\tau(p, q) = \frac{\tau^p}{p}\, {}_2F_1(p,\, 1-q;\, p+1;\, \tau)$$

the parameterization (3) can be rewritten in the form [15]

$$z(x) = \frac{r}{n+2}{}_2F_1(\frac{n+2}{2n+2},\, \frac{1}{2};\, \frac{3n+4}{2n+2};\, 1) - \frac{x^{n+2}}{(n+2)r^{n+1}}\, {}_2F_1(\frac{n+2}{2n+2},\, \frac{1}{2};\, \frac{3n+4}{2n+2};\, \tau(x)). \tag{4}$$

Relying on another useful relation

$${}_2F_1(\alpha, \beta; \gamma; 1) = \frac{\Gamma(\gamma)\Gamma(\gamma-\alpha-\beta)}{\Gamma(\gamma-\alpha)\Gamma(\gamma-\beta)}$$

connecting ${}_2F_1(\alpha, \beta; \gamma; 1)$ with the *gamma function*

$$\Gamma(\zeta) = \int_0^\infty t^{\zeta-1}\mathrm{e}^{-t}\mathrm{d}t, \qquad \zeta \in \mathbb{C}, \qquad \mathrm{Re}\,\zeta > 0 \tag{5}$$

the representation (4) of the profile curve can be transformed also in the form [15]

$$z(x) = \frac{r\,\sqrt{\pi}\,\Gamma\left(\frac{n+2}{2n+2}\right)}{2(n+1)\Gamma\left(\frac{2n+3}{2n+2}\right)} - \frac{x^{n+2}}{(n+2)r^{n+1}}\, {}_2F_1(\frac{n+2}{2n+2},\, \frac{1}{2};\, \frac{3n+4}{2n+2};\, \tau(x)).$$

The Gamma function is an extension of the factorial operation to complex numbers given by the formula $\zeta\,! = \Gamma(\zeta + 1)$. In the derivation of the above formulas we

have availed of its special value $\Gamma(1/2) = \sqrt{\pi}$ and the recurrence relation

$$\Gamma(1) = 1, \qquad \Gamma(\zeta + 1) = \zeta\,\Gamma(\zeta).$$

In the next sections (after some preliminaries on the differential geometry of surfaces), a collection of alternative parameterizations of $LW(1)$ (Section 3) and $LW(2)$ balloons (Section 4) are presented. Some geometrical characteristics of these surfaces are given as well (Section 5).

## 2. Some Preliminaries on the Geometry of Surfaces

A parameterized surface $\mathcal{S} \subset \mathbb{R}^3$

$$\mathbf{x}(u, v) = (x(u, v), y(u, v), z(u, v)), \qquad (u, v) \in U \subset \mathbb{R}^2$$

is determined almost uniquely by its first $I$ and second $II$ fundamental forms [18]

$$I = E\mathrm{d}u^2 + 2F\mathrm{d}u\mathrm{d}v + G\mathrm{d}v^2, \qquad II = L\mathrm{d}u^2 + 2M\mathrm{d}u\mathrm{d}v + N\mathrm{d}v^2$$

where the coefficients are defined by the formulas

$$\begin{gathered} E = \mathbf{x}_u \cdot \mathbf{x}_u, \qquad F = \mathbf{x}_u \cdot \mathbf{x}_v, \qquad G = \mathbf{x}_v \cdot \mathbf{x}_v \\ L = \mathbf{x}_{uu} \cdot \mathbf{n}, \qquad M = \mathbf{x}_{uv} \cdot \mathbf{n}, \qquad N = \mathbf{x}_{vv} \cdot \mathbf{n} \end{gathered} \tag{6}$$

and $\mathbf{n}$ is the unit vector which is normal to the surface $\mathcal{S}$

$$\mathbf{n} = \frac{\mathbf{x}_u \times \mathbf{x}_v}{|\mathbf{x}_u \times \mathbf{x}_v|}.$$

Here, we have used the standard notation $\mathbf{x}_u = \partial\mathbf{x}/\partial u$, $\mathbf{x}_{uu} = \partial^2\mathbf{x}/\partial u^2$, etc. The mean $H$ and the Gaussian $K$ curvatures of the surface are calculated by the classical formulas (cf. [18])

$$H = \frac{EN + GL - 2FM}{2(EG - F^2)}, \qquad K = \frac{LN - M^2}{EG - F^2}.$$

The parallel $k_\pi$ and the meridional $k_\mu$ principal curvatures are related with $H$ and $K$ through the equations $H = (k_\pi + k_\mu)/2$ and $K = k_\pi k_\mu$, whereby

$$k_\mu = H + \sqrt{H^2 - K}, \qquad k_\pi = H - \sqrt{H^2 - K}.$$

If $\mathcal{S}$ is a surface of revolution given by

$$\mathbf{x}(u, v) = (h(u)\cos v, h(u)\sin v, g(u))$$

then its principal curvatures can be found via the classical formulas

$$k_\pi = \frac{g'}{h(g'^2 + h'^2)^{1/2}}, \qquad k_\mu = \frac{g''h' - g'h''}{(g'^2 + h'^2)^{3/2}} \tag{7}$$

where $g' \equiv \mathrm{d}g/\mathrm{d}u$, etc.

## 3. The Mylar Balloon

The Mylar balloon is the *LW*$(1)$ balloon – the second representative of the *LW*$(n)$ class of surfaces (the first one being the sphere for $n = 0$) that according to the definition (1) obeys the relation

$$k_\mu = 2k_\pi.$$

The name "Mylar balloon" was coined in [21] by Paulsen, as the shape of this surface almost perfectly approaches the shape of the balloon made of two sewn together circular disks of the Mylar® foil. Paulsen had observed that the obtained Euler-Lagrange equation has no closed form solution in elementary functions. The first fully analytical description of the Mylar balloon was presented in [9] in the form

$$\begin{aligned} &x(u,v) = r\cos u\cos v, \quad y(u,v) = r\cos u\sin v \\ &z(u,v) = r\sqrt{2}[E(u,\frac{1}{\sqrt{2}}) - \frac{1}{2}F(u,\frac{1}{\sqrt{2}})], \qquad u \in [-\frac{\pi}{2},\frac{\pi}{2}],\ v \in (0,2\pi] \end{aligned} \tag{8}$$

where

$$\begin{aligned} F(\varphi,k) \,&=\, u_1 = \int\limits_0^\varphi \frac{\mathrm{d}t}{\sqrt{1-k^2\sin^2 t}} \\ E(\varphi,k) \,&=\, E(\mathrm{am}\,u_1,k) = \int\limits_0^\varphi \sqrt{1-k^2\sin^2 t}\,\mathrm{d}t \end{aligned} \tag{9}$$

are the *normal elliptic integrals* of the first and the second kind, respectively, with argument $\varphi$ and modulus $k$ (for more details see [3]). The function

$$\varphi = \mathrm{am}\,u_1 \equiv \mathrm{am}\,(u_1,k) \tag{10}$$

is the so-called Jacobian *elliptic amplitude function*, defined as the inverse of the first kind elliptic integral $F(\varphi,k)$. For the coefficients of the first and the second fundamental forms the machinery of the differential geometry, after lengthy

computations, produce the result [9]

$$E = \frac{r^2}{1+\cos^2 u}, \qquad F = 0, \qquad G = r^2\cos^2 u$$

$$L = \frac{2r\cos u}{1+\cos^2 u}, \qquad M = 0, \qquad N = r\cos^3 u.$$

Then it is quite easy to obtain the two principal curvatures

$$k_\mu = \frac{2\cos u}{r}, \qquad k_\pi = \frac{\cos u}{r}$$

and respectively the mean and the Gaussian curvatures are given by the formulas

$$H = \frac{3\cos u}{2r}, \qquad K = \frac{2\cos^2 u}{r^2}.$$

As it has been shown in [13] (see also [16, 20]), by making use again of the *Jacobian elliptic functions*, the representation (8) can be rewritten in the form

$$\begin{aligned} x(u,v) &= r\,\mathrm{cn}(u,\tfrac{1}{\sqrt{2}})\cos v, \qquad y(u,v) = r\,\mathrm{cn}(u,\tfrac{1}{\sqrt{2}})\sin v \\ z(u,v) &= r\sqrt{2}[E(\mathrm{sn}(u,\tfrac{1}{\sqrt{2}}),\tfrac{1}{\sqrt{2}}) - \frac{1}{2}F(\mathrm{sn}(u,\tfrac{1}{\sqrt{2}}),\tfrac{1}{\sqrt{2}})] \end{aligned} \tag{11}$$

in which $u \in [-K(1/\sqrt{2}), K(1/\sqrt{2})]$, $v \in (0, 2\pi]$, and where $\mathrm{sn}\,(u,\,k)$, $\mathrm{cn}\,(u,\,k)$ and $K(k)$ denote the *sine* and the *cosine* Jacobian elliptic functions

$$\mathrm{sn}\,(u,\,k) = \sin(\mathrm{am}\,(u,\,k)), \qquad \mathrm{cn}\,(u,\,k) = \cos(\mathrm{am}\,(u,\,k))$$

and respectively, the *complete elliptic integral* of the first kind

$$K(k) = F\left(\frac{\pi}{2}, k\right) = \int_0^{\pi/2} \frac{\mathrm{d}t}{\sqrt{1-k^2\sin^2 t}}.$$

Then, the corresponding coefficients of the first and the second fundamental forms are given by the expressions [13]

$$E = \frac{r^2}{2}, \qquad F = 0, \qquad G = r^2\,\mathrm{cn}^2(u,\tfrac{1}{\sqrt{2}})$$

$$L = r\,\mathrm{cn}(u,\tfrac{1}{\sqrt{2}}), \qquad M = 0, \qquad N = r\,\mathrm{cn}^3(u,\tfrac{1}{\sqrt{2}})$$

and the principal, the mean and the Gaussian curvatures are respectively

$$k_\mu = \frac{2\mathrm{cn}\big(u,\, 1/\sqrt{2}\big)}{r}, \qquad k_\pi = \frac{\mathrm{cn}\big(u,\, 1/\sqrt{2}\big)}{r}$$

$$H = \frac{3\mathrm{cn}\big(u,\, 1/\sqrt{2}\big)}{2r}, \qquad K = \frac{2\mathrm{cn}^2\big(u,\, 1/\sqrt{2}\big)}{r^2}.$$

By introducing *isothermal* (*conformal*) *coordinates* $(u, v)$, the parameterization of the Mylar balloon takes the form [10, 11]

$$\begin{aligned} x(u,v) &= \frac{r}{\sqrt{\cosh 2u}}\cos v, \qquad y(u,v) = \frac{r}{\sqrt{\cosh 2u}}\sin v, \\ z(u,v) &= \sqrt{2}r[E(\frac{\sqrt{2}\sinh u}{\sqrt{\cosh 2u}}, \frac{1}{\sqrt{2}}) - \frac{1}{2}F(\frac{\sqrt{2}\sinh u}{\sqrt{\cosh 2u}}, \frac{1}{\sqrt{2}})] \end{aligned} \tag{12}$$

where $u \in (-\infty, \infty)$, $v \in [0, 2\pi]$. The corresponding fundamental forms are

$$I = \frac{r^2}{\cosh 2u}\,(\mathrm{d}u^2 + \mathrm{d}v^2), \qquad II = \frac{r}{\cosh^{3/2} 2u}\,(2\,\mathrm{d}u^2 + \mathrm{d}v^2).$$

In *Whewell representation* the profile curve of the Mylar balloon is given by the formulas (see [6])

$$\begin{aligned} x(\theta) &= r\sqrt{\sin\theta} \\ z(\theta) &= \sqrt{2}r[E(\arccos\sqrt{\sin\theta}, \frac{1}{\sqrt{2}}) - \frac{1}{2}F(\arccos\sqrt{\sin\theta}, \frac{1}{\sqrt{2}}] \end{aligned} \tag{13}$$

where $\theta \in [0, \pi]$ is the angle between the tangent line to the profile curve and the $OX$-axis. Another alternative parameterization of the Mylar balloon has been obtained in [22] by employing the *Weierstrassian functions*

$$\begin{aligned} x(u,v) &= r\frac{2\wp(u) - r^2}{2\wp(u) + r^2}\cos v, \qquad y(u,v) = r\frac{2\wp(u) - r^2}{2\wp(u) + r^2}\sin v \\ z(u,v) &= 2\zeta(u) + \frac{2\wp'(u)}{2\wp(u) + r^2}, \qquad u \in \left[-\frac{\tilde{\omega}}{2r}, \frac{\tilde{\omega}}{2r}\right], \qquad v \in (0, 2\pi] \end{aligned} \tag{14}$$

where $\wp(u) \equiv \wp(u; -r^4, 0)$, $\wp'(u) \equiv \wp'(u; -r^4, 0)$ and $\zeta(u) \equiv \zeta(u; -r^4, 0)$ are respectively the Weierstrassian $\wp$-function $\wp(u)$, its derivative $\wp'(u)$ and the Weierstrassian zeta function $\zeta(u)$ built with the invariants [1, 25]

$$g_2 = -r^4, \qquad g_3 = 0$$

and $\tilde{\omega}$ is the *lemniscate constant*

$$\tilde{\omega} \approx 2.6220.$$

The basic geometrical characteristics of the Mylar balloon in terms of the Weierstrassian functions are as follows [22]. The coefficients of the first fundamental form are

$$E = r^4, \qquad F = 0, \qquad G = r^2 \left( \frac{2\wp(u) - r^2}{2\wp(u) + r^2} \right)^2$$

and that ones of the second fundamental form are respectively

$$L = 2r^3 \left( \frac{2\wp(u) - r^2}{2\wp(u) + r^2} \right), \qquad M = 0, \qquad N = r \left( \frac{2\wp(u) - r^2}{2\wp(u) + r^2} \right)^3.$$

Therefore, one can easily find the mean and the Gaussian curvatures

$$H = \frac{3}{2r} \left( \frac{2\wp(u) - r^2}{2\wp(u) + r^2} \right), \qquad K = \frac{2}{r^2} \left( \frac{2\wp(u) - r^2}{2\wp(u) + r^2} \right)^2$$

along with the principal curvatures

$$k_\mu = \frac{2}{r} \left( \frac{2\wp(u) - r^2}{2\wp(u) + r^2} \right), \qquad k_\pi = \frac{1}{r} \left( \frac{2\wp(u) - r^2}{2\wp(u) + r^2} \right).$$

In this section we have presented the $LW(1)$ balloon (the Mylar balloon) by introducing five alternative parameterizations (8), (11), (12), (13) and (14) derived elsewhere by making use of the elliptic functions and elliptic integrals.

## 4. The $LW(2)$ Balloon

The $LW(2)$ balloon is the third representative of the $LW(n)$ surfaces defined uniquely by the relation

$$k_\mu = 3k_\pi. \tag{15}$$

From some other perspective, the $LW(2)$ balloon coincides with the surface of revolution formed by the *rotating liquid drop* – an equilibrium state of an incompressible fluid mass subjected to a surface tension and rotated with constant angular velocity about a fixed axis of revolution. The outer surfaces of such rotating liquid

drops as shown in [12, 17], belong to the class of linear Weingarten surfaces of revolution for which

$$k_\mu = 3k_\pi + c, \qquad c \in \mathbb{R}. \tag{16}$$

Accordingly, the $LW(2)$ balloon is obtained for $c = 0$. Six parameterizations of the profile curves of the $LW(2)$ balloon starting with

$$\gamma(u) = (h(u), 0, g(u))$$

will be obtained below and now we proceed with their description.

### 4.1. Monge Parameterization

Let us start with the Monge parameterization, viz., $h(u) = u \equiv x$

$$\gamma(x) = (x, 0, g(x))$$

and relying to equation (7) we get the expressions

$$k_\pi = \frac{g'}{x(1+g'^2)^{1/2}}, \qquad k_\mu = \frac{\mathrm{d}(xk_\pi)}{\mathrm{d}x}.$$

Then, by imposing the condition (15) the principal curvatures of the $LW(2)$ surface take the form

$$k_\pi = \frac{x^2}{r^3}, \qquad k_\mu = \frac{3x^2}{r^3}, \qquad r > 0$$

and the function $g(x)$ is expressed by the elliptic integral

$$g(x) = \frac{r}{2} \int\limits_{(x/r)^2}^{1} \frac{t\mathrm{d}t}{\sqrt{1-t^3}}. \tag{17}$$

Passing to the canonical representation of the latter integral (cf. formulas (9) and the handbook [3]) we arrive at the *Monge parameterization*

$$z(x) = r\Big(\frac{\sqrt{3}-1}{2\sqrt[4]{3}} F(\varphi(x), k) - \sqrt[4]{3}\, E(\varphi(x), k) + \frac{\sqrt{1-(x/r)^6}}{1+\sqrt{3}-(x/r)^2}\Big)$$

$$\varphi(x) = \arccos \frac{\sqrt{3}-1+(x/r)^2}{\sqrt{3}+1-(x/r)^2}, \qquad k = \frac{\sqrt{2+\sqrt{3}}}{2}, \qquad x \in [0, r]. \tag{18}$$

Note that the profile curve, parameterized by (18), is traced counterclockwise from S (the South Pole corresponding to $x \equiv 0$), to the equator E (where $x \equiv r$).

### 4.2. Parameterization Via the Amplitude

The second parameterization of the profile curve of the considered Weingarten surface $LW(2)$ is derived from (18) by taking the *elliptic amplitude* $\varphi$ as a parameter, viz., $u \equiv \varphi = \operatorname{am} u_1$ (cf. (10))

$$
\begin{aligned}
x(\varphi) &= r\sqrt{\frac{1-\sqrt{3}+(1+\sqrt{3})\cos\varphi}{1+\cos\varphi}} \\
z(\varphi) &= r\Big(\frac{1-\sqrt{3}}{2\sqrt[4]{3}}F(\varphi,k)+\sqrt[4]{3}\,E(\varphi,k)-\frac{\sqrt[4]{3}\sin\varphi\sqrt{1-k^2\sin^2\varphi}}{1+\cos\varphi}\Big) \qquad (19)\\
&\varphi\in[-\arccos\frac{\sqrt{3}-1}{\sqrt{3}+1},\ \arccos\frac{\sqrt{3}-1}{\sqrt{3}+1}t], \qquad k=\frac{\sqrt{2+\sqrt{3}}}{2}.
\end{aligned}
$$

The profile curve obtained by (19) is traced counterclockwise starting from the South Pole S, running through the whole range of the amplitude, with $\varphi = 0$ at the equator E, and ending at the North Pole N.

The coefficients of the first fundamental form of the balloon, corresponding to the *elliptic amplitude parameterization* (19), follow directly by applying the definition (6)

$$
\begin{aligned}
E &= \frac{4r^2\cos^2(\varphi/2)}{\sqrt{3}\left(\left(1+\sqrt{3}\right)\cos\varphi-\sqrt{3}+1\right)\left(\left(2+\sqrt{3}\right)\cos 2\varphi-\sqrt{3}+6\right)}\\
F &= 0, \qquad G=\frac{r^2\left(\left(1+\sqrt{3}\right)\cos\varphi-\sqrt{3}+1\right)}{\cos\varphi+1}.
\end{aligned}
$$

### 4.3. Arclength Related Parameterization

We start with a parameterization of the profile curve, performed with respect to the arclength parameter $s$, viz. $u \equiv s$

$$\gamma(s) = (h(s), 0, g(s))$$

so that the coordinate functions

$$x = h(s), \qquad z = g(s)$$

satisfy the Frenet-Serret equations

$$\ddot{x} - \frac{3x^2}{r^3}\dot{z} = 0, \qquad \ddot{z} + \frac{3x^2}{r^3}\dot{x} = 0 \qquad (20)$$

where the curvature $k$ of $\gamma$ is taken to be equal to the principal curvature $k_\mu$ of $\mathcal{S}$ (as $\gamma$ is actually a meridional curve)

$$k \equiv k_\mu = \frac{3x^2}{r^3}\cdot$$

Here and henceforth, the differentiation with respect to the arclength parameter is denoted by dots: $\dot{x} \equiv \mathrm{d}x/\mathrm{d}s$, etc. By integrating once, the system (20) takes the form

$$\dot{x}^2 = -\frac{x^6}{r^6} + 1, \qquad \dot{z} = -\frac{x^3}{r^3}\cdot \tag{21}$$

In obtaining the above equations we have considered the unit speed equation

$$\dot{x}^2 + \dot{z}^2 = 1$$

and the transversality condition at $x = 0$ (cf. Section 1). We proceed with the integration of the system (21) in terms of the Weierstrassian functions. From (21) we deduce

$$\frac{\mathrm{d}z}{\mathrm{d}x} = -\frac{x^3}{\sqrt{r^6 - x^6}} \tag{22}$$

and then by introducing the new variables $\tilde{s}$ and $\chi$ on writing

$$\chi = -\frac{x^2}{4r^2}, \qquad \frac{\mathrm{d}\chi}{\mathrm{d}\tilde{s}} = \sqrt{4\chi^3 + \frac{1}{16}} \tag{23}$$

the equation (22) is transformed to

$$\frac{\mathrm{d}z}{\mathrm{d}\tilde{s}} = -2r\chi(\tilde{s}). \tag{24}$$

The second equation in (23) is equivalent to the relation

$$\chi(\tilde{s}) = \wp(\tilde{s} + C;\, 0, -1/16), \qquad C \in \mathbb{R}$$

connecting $\chi$ with the Weierstrassian $\wp$-function [25]. The solution of the equation (24) is now readily expressed by the help of the Weierstrassian $\zeta$-function, resulting in a parameterization via the *arclength related parameter* $\tilde{s}$ ($C = 0$)

$$x(\tilde{s}) = 2r\sqrt{-\wp(\tilde{s})}, \qquad z(\tilde{s}) = 2r\,\zeta(\tilde{s}), \qquad \tilde{s} \in [0, 2\pi) \tag{25}$$

where $\wp(\tilde{s}) \equiv \wp(\tilde{s};\, 0, -1/16)$ and $\zeta(\tilde{s}) \equiv \zeta(\tilde{s};\, 0, -1/16)$. It should be remembered that the two parameters $s$ and $\tilde{s}$ are related (implicitely) through the differential connection

$$\left(\frac{\mathrm{d}\tilde{s}}{\mathrm{d}s}\right)^2 = -\frac{16\wp(\tilde{s})}{r^2}$$

which is readily obtained by substituting the solution (25) in either one of the two equations of the system (21). The first and the second fundamental forms follow by direct calculation

$$E = -\frac{r^2}{16\,\wp(\tilde{s})}, \qquad F = 0, \qquad G = -4r^2\,\wp(\tilde{s})$$

$$L = \frac{3r}{4}, \qquad M = 0, \qquad N = 16r\,\wp^2(\tilde{s}).$$

### 4.4. Whewell Parameterization

The fourth parameterization of the $LW(2)$ is accomplished by taking the $u$-parameter to be the angle $\theta$ between the tangent line to the profile curve $\gamma$ and the $OX$-axis, viz. $u = \theta$

$$\gamma(\theta) = (h(\theta), 0, g(\theta)).$$

In order to obtain the coordinate functions $h(\theta)$ and $g(\theta)$ we at first integrate once the second one of the Frenet-Serret equations (20)

$$\dot{z} = -\frac{x^3}{r^3} \tag{26}$$

and combining the so obtained expression with the second one of the two defining equations for the angle $\theta$

$$\dot{x} = \cos\theta, \qquad \dot{z} = \sin\theta \tag{27}$$

we arrive at the desired expression for the $x$-coordinate of $\gamma$

$$x = h(\theta) = -r\sqrt[3]{\sin\theta}. \tag{28}$$

On the other hand, from (27) it follows the relation

$$\ddot{x} = -\dot{\theta}\dot{z}$$

which together with the first one of the Frenet-Serret equations (20) immediately leads to

$$\dot{\theta} = -\frac{3x^2}{r^3}\cdot \tag{29}$$

Then, on writing

$$\frac{\mathrm{d}z}{\mathrm{d}\theta} = \frac{\dot{z}}{\dot{\theta}}$$

and substituting with (26) and (29) it is straightforward to obtain the following integral representation of the $z$-coordinate of $\gamma$

$$z = g(\theta) = -\frac{r}{3}\int\limits_{\theta}^{\pi/2} \sqrt[3]{\sin\tau}\,\mathrm{d}\tau.$$

Under the change of the integration variable

$$t = \sqrt[3]{\sin^2 \tau}$$

this latter integral is reduced to the same elliptic integral found previously with regard to the Monge representation (cf. formula (17))

$$g(\theta) = -\frac{r}{2} \int\limits_{\sqrt[3]{\sin^2 \theta}}^{1} \frac{t\mathrm{d}t}{\sqrt{1-t^3}}. \tag{30}$$

Finally, by carrying out the process of reduction to canonical elliptic integrals as in Section 4.1, the *Whewell parameterization* of the profile curve $\gamma$ of the *LW*$(2)$ balloon takes the form

$$\begin{aligned} x(\theta) &= r\sqrt[3]{\sin\theta} \\ z(\theta) &= r\Big(\frac{\sqrt{3}-1}{2\sqrt[4]{3}} F(\varphi(\theta),k) - \sqrt[4]{3}\, E(\varphi(\theta),k) + \frac{\cos\theta}{1+\sqrt{3}-\sqrt[3]{\sin^2\theta}}\Big) \qquad (31) \\ \varphi(\theta) &= \arccos\frac{\sqrt{3}-1+\sqrt[3]{\sin^2\theta}}{\sqrt{3}+1-\sqrt[3]{\sin^2\theta}}, \qquad k = \frac{\sqrt{2+\sqrt{3}}}{2}, \qquad \theta \in \Big[0, \frac{\pi}{2}\Big] \end{aligned}$$

where $x$ has been replaced by $-x$ (cf. the minus sign in (28)). We should note that the parameterization (31) can be obtained directly by combining the formulas (18) and (28).

The profile curve parameterized by (31) is traced counterclockwise from $S$ (the South Pole corresponding to $\theta \equiv 0$) to the equator $E$ (where $\theta \equiv \pi/2$).

### 4.5. Alternative Whewell Parameterization

The integral in (30) can be also expressed via the so-called *Gaussian hypergeometric function* ${}_2F_1(\,a,\,b;\,c;\,\zeta)$ [1], resulting in another representation of the profile curve via the tangential angle $\theta$ – *an alternative Whewell parameterization*

$$x(\theta) = r\sqrt[3]{\sin\theta}, \quad z(\theta) = -\frac{r\cos\theta}{3}\,{}_2F_1\Big(\frac{1}{2},\,\frac{1}{3};\,\frac{3}{2};\,\cos^2\theta\Big), \quad \theta \in [0,\pi] \tag{32}$$

and the formulas ensued for the geometrical characteristics of the *LW*$(2)$ balloon. Starting with the first and second fundamental forms

$$E = \frac{r^2}{9\sin^{4/3}\theta}, \qquad F = 0, \qquad G = r^2\sin^{2/3}\theta$$

$$L = -\frac{r}{3\sin^{2/3}\theta}, \qquad M = 0, \qquad N = -r\sin^{4/3}\theta$$

one easily finds the principal curvatures

$$k_\pi = -\frac{\sin^{2/3}\theta}{r}, \qquad k_\mu = -\frac{3\sin^{2/3}\theta}{r}$$

and then the mean and the Gaussian curvatures

$$H = -\frac{2\sin^{2/3}\theta}{r}, \qquad K = \frac{3\sin^{4/3}\theta}{r^2}, \qquad H^2 - K = \frac{\sin^{4/3}\theta}{r^2}.$$

The profile curve, parameterized by (32), is traced counterclockwise from the South Pole S ($\theta = 0$) through the equator E ($\theta \equiv \pi/2$) to the North Pole N ($\theta \equiv \pi$).

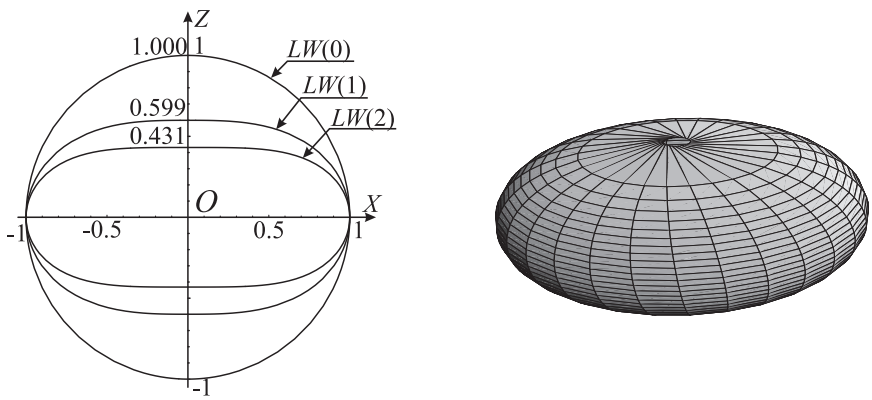


**Figure 2.** The profile curves of three linear Weingarten surfaces of revolution with radius $r = 1$. From outside in, the sphere *LW*$(0)$ with $k_\mu/k_\pi = 1$, the Mylar balloon *LW*$(1)$ with $k_\mu/k_\pi = 2$ and the *LW*$(2)$ balloon with $k_\mu/k_\pi = 3$. Right: 3D view of the *LW*$(2)$ balloon.

### 4.6. Isothermal Parameterization

In the sixth parameterization of the considered *LW*$(2)$ surface, we introduce an *isothermal* coordinate system $(u, v)$ on $\mathcal{S}$ by imposing the relation with the tangential angle $\theta$

$$\sin\theta\cosh 3u = 1 \tag{33}$$

leading us to the following integral representation of the profile curve $\gamma$ of *LW*$(2)$

$$x(u) = \frac{r}{\sqrt[3]{\cosh 3u}}, \qquad z(u) = r\int_0^u \frac{\mathrm{d}t}{\cosh 3t\,\sqrt[3]{\cosh 3t}}, \qquad u \in (-2\pi, 2\pi)$$

(compare with the formulas in Section 4.4 and Section 4.5). By substituting for $\sin\theta$ from (33) into the Whewell representation (31), we arrive at an explicit *isothermal parameterization* of the *LW*$(2)$ balloon, i.e.,

$$x(u,v)=\frac{r}{\sqrt[3]{\cosh 3u}}\cos v, \qquad y(u,v)=\frac{r}{\sqrt[3]{\cosh 3u}}\sin v$$

$$z(u,v)=r\Big(\frac{1-\sqrt{3}}{2\sqrt[4]{3}}F(\varphi(u),k)+\sqrt[4]{3}E(\varphi(u),k)-\frac{\sinh 3u}{(1+\sqrt{3})\cosh 3u-\sqrt[3]{\cosh 3u}}\Big) \quad (34)$$

$$\varphi(u)=\arccos\frac{(\sqrt{3}-1)\sqrt[3]{\cosh^2 3u}+1}{(\sqrt{3}+1)\sqrt[3]{\cosh^2 3u}-1}, \qquad k=\frac{\sqrt{2+\sqrt{3}}}{2}, \qquad u\in[0,2\pi]$$

for which the first and second fundamental forms are given by

$$I=\frac{r^2}{\cosh^{2/3}3u}(\mathrm{d}u^2+\mathrm{d}v^2), \qquad II=\frac{r}{\cosh^{4/3}3u}(3\mathrm{d}u^2+\mathrm{d}v^2).$$

When parameterized by (34) the profile curve of the *LW*$(2)$ balloon is traced counterclockwise starting from the equator (for $u\equiv 0$) and reaching to the North Pole where $u\equiv 2\pi$.

Thus far, we have presented a pure geometrical depiction of the *LW*$(2)$ balloon in terms of elliptic and Gaussian hypergeometric special functions. The *LW*$(2)$ balloon is the third representative of a class of linear Weingarten surfaces *LW*$(n)$ which principal curvatures obey the relation $k_\mu=(n+1)k_\pi$. The profile curves of the first three surfaces obtained for $n=0,1,2$ are plotted in Fig. 2 together with a 3D view of the *LW*$(2)$ balloon, both of them drawn by *Mathematica*®. In the next section some geometric and compactness measures of these three balloons are evaluated and compared.

## 5. Metric Relations and Compactness Measures

Having the explicit parameterizations of the *LW*$(1)$ (Section 3) and the *LW*$(2)$ (Section 4) balloons, we calculated some truly geometric quantities – the circumference $l=4a$ of the profile curve, the thickness $\tau$, the area $\Sigma$ of the meridional section, the surface area $A$ and the volume $V$, characterizing the surfaces via metric relations (Table 1 and Table 2), and two other quantities – sphericity and homogeneity, indicating for the compactness of their shapes (Table 3).

From the approximate numerical values (in the right sides of the tables), it is seen that, with the increase of $n$, all the characteristic measures monotonically decline, which is clearly confirmed by the plots of the three, placed in each other (starting from the sphere) profile curves (Fig. 2).

Details about the derivation of the metric dependencies for the *LW*(1) balloon versus $r$ (cf. Fig. 1) can be found in [6,9,11,13,22]. By making similar operations for the *LW*(2) balloon we ended up with expressions in Table 1 and Table 2, involving the gamma function (cf. formula (5)). We should mention that in his investigation of the Mylar balloon (*LW*(1)) Paulsen [21] has expressed $l$, $\tau$ and $V$ via the gamma function, i.e.,

$$\frac{l}{2r}=\frac{\Gamma^2(1/4)}{2\sqrt{2\pi}},\qquad \frac{\tau}{2r}=\frac{\sqrt{2}\,\pi^{3/2}}{\Gamma^2(1/4)},\qquad \frac{V}{r^3}=\frac{\sqrt{\pi}\,\Gamma^2(1/4)}{6\sqrt{2}}.$$

Yet, given that for *LW*(1) the Euler-Lagrange equation (2) is directly reduced to elliptic integral, it is quite natural to expect that the most compact expressions for this surface can be obtained in terms of elliptic integrals and elliptic functions (cf. Section 3 and the papers cited therein). Here are three of the characteristics measures for *LW*(1) in all of which the factor $K\left(1/\sqrt{2}\right)$ is present

$$\frac{l}{2r}=\sqrt{2}\,K\left(\frac{1}{\sqrt{2}}\right),\qquad \frac{\tau}{2r}=\frac{\pi}{2\sqrt{2}\,K\left(1/\sqrt{2}\right)},\qquad \frac{V}{r^3}=\frac{\pi\sqrt{2}}{3}K\left(\frac{1}{\sqrt{2}}\right).$$

**Table 1.** Two characteristic measures of the *LW*(*n*) balloons ($n=0,1,2$) versus the diameter $2r$ for the circumference $l$ and the thickness $\tau$ of the profile curve. Right: Approximate values.

| | *LW*(0) | *LW*(1) | *LW*(2) |
|---|---|---|---|
| $l/2r$ | $\pi$ | $\tilde{\omega}$ | $\frac{\sqrt{\pi}\,\Gamma\left(\frac{1}{6}\right)}{3\,\Gamma\left(\frac{2}{3}\right)}$ |
| $\tau/2r$ | 1 | $\frac{\pi}{2\tilde{\omega}}$ | $\frac{\sqrt{\pi}\,\Gamma\left(\frac{2}{3}\right)}{6\,\Gamma\left(\frac{7}{6}\right)}$ |

| | *LW*(0) | *LW*(1) | *LW*(2) |
|---|---|---|---|
| $l/2r$ | 3.1416 | 2.6220 | 2.4286 |
| $\tau/2r$ | 1 | 0.5991 | 0.4312 |

The constant that plays a key role in the whole description of the *LW*(1) balloon and most contributes for the compactness of the expressions is the lemniscate constant $\tilde{\omega}$ (for more details see [22]). By comparing the above expressions with those for the *LW*(1) in Table 1 and Table 2, a chain of connections between the lemniscate constant and certain values of the special functions $K(k)$ and $\Gamma(\zeta)$ is obtained (see [1])

$$\frac{\tilde{\omega}}{\sqrt{2}}=K\left(\frac{1}{\sqrt{2}}\right)=\frac{\Gamma^2(1/4)}{4\sqrt{\pi}}.$$

From Table 2 we observe also that the volume of the *LW*(2) balloon diminishes twice, compared to the volume of the sphere, and the three volumes are related as follows

$$V_0\,:\,V_1\,:\,V_2=4\,:\,\tilde{\omega}\,:\,2.$$

**Table 2.** Three characteristic measures of the *LW*(*n*) balloons ($n = 0, 1, 2$) versus the radius $r$. The area of the meridional section $\Sigma$, the surface area $A$ and the volume $V$. Right: Approximate values.

| | *LW*(0) | *LW*(1) | *LW*(2) |
|---|---|---|---|
| $\Sigma/r^2$ | $\pi$ | $2$ | $\frac{2\sqrt{\pi}\,\Gamma\left(\frac{5}{6}\right)}{3\,\Gamma\left(\frac{4}{3}\right)}$ |
| $A/r^2$ | $4\pi$ | $\pi^2$ | $\frac{2\pi^{3/2}\,\Gamma\left(\frac{1}{3}\right)}{3\,\Gamma\left(\frac{5}{6}\right)}$ |
| $V/r^3$ | $\frac{4}{3}\pi$ | $\frac{1}{3}\pi\tilde{\omega}$ | $\frac{2}{3}\pi$ |

| | *LW*(0) | *LW*(1) | *LW*(2) |
|---|---|---|---|
| $\Sigma/r^2$ | 3.1416 | 2 | 1.4937 |
| $A/r^2$ | 12.5664 | 9.8696 | 8.8102 |
| $V/r^3$ | 4.1888 | 2.7457 | 2.0944 |

From Table 3 one can track the change of two compactness measures – sphericity and homogeneity applied to the *LW*(*n*) surfaces, according to their definitions: given an arbitrary surface $\mathcal{S}$ with surface area $A$ and volume $V$, the *sphericity* $\Psi$ is the ratio of the surface area of a sphere of the same volume $V$, to the surface area $A$ and the *homogeneity* $\Theta$ is the ratio of the volume of a sphere of the same surface area $A$ to the volume $V$

$$\Psi = \frac{\sqrt[3]{36\,\pi}\,V^{2/3}}{A}, \qquad \Theta = \frac{A^{3/2}}{6\sqrt{\pi}\,V}.$$

The "compactness" measures have important practical use. Sphericity was introduced by Wadell in 1935 [24] in order to evaluate how closely the shape of an object approaches that of the "mathematically perfect object" – the sphere.
For example, sphericity of the balls inside a ball bearing is used as a measure for the quality of the bearing, such as the load it can bear or the speed at which it can turn without failing.

**Table 3.** Compactness measures (sphericity $\Psi$ and homogeneity $\Theta$) for the *LW*(*n*) balloons, $n = 0, 1, 2$. Right: Their approximate values.

| | *LW*(0) | *LW*(1) | *LW*(2) |
|---|---|---|---|
| $\Psi$ | 1 | $\frac{(2\tilde{\omega})^{2/3}}{\pi}$ | $\frac{3\,\sqrt[3]{2}\,\Gamma\left(\frac{5}{6}\right)}{\sqrt{\pi}\,\Gamma\left(\frac{1}{3}\right)}$ |
| $\Theta$ | 1 | $\frac{\pi^{3/2}}{2\tilde{\omega}}$ | $\frac{\pi^{3/4}\left[\Gamma\left(\frac{1}{3}\right)\right]^{3/2}}{3\sqrt{6}\left[\Gamma\left(\frac{5}{6}\right)\right]^{3/2}}$ |

| | *LW*(0) | *LW*(1) | *LW*(2) |
|---|---|---|---|
| $\Psi$ | 1 | 0.9608 | 0.8985 |
| $\Theta$ | 1 | 1.0618 | 1.1741 |

As it can be inferred from the definitions, and clearly seen from the approximate values in Table 3, the sphericity and the homogeneity act in a "reciprocal" way: while the values of $\Psi$ become smaller (with increasing of $n$), $\Theta$ acquires larger values. This is obviously due to the fact that, in view of the shape of the *LW*($n$) surfaces (cf. Fig. 2), the sequence of the surface areas $\{A_n\}_{n=0}^{\infty}$ is bounded by $2\pi r^2$, while the sequence of volumes $\{V_n\}_{n=0}^{\infty}$ vanishes when $n$ goes to infinity.

## Conclusion

Here we have presented explicit parameterizations of the linear Weingarten surfaces *LW*(n) for $n = 0, 1, 2$. While the first two are well documented in the literature the third one is relatively new. Besides the purely geometrical interest in this surface it should be noted that the *LW*(2) balloon presents an example (together with the sphere and the right circular cylinder) of the surface which can be deformed by uniform pressure without bending [8]. One should point out that this is not of entirely academic interest as there are many instances in practice in which one looks for a flexible but inextensible membrane of a specified shape, which is to be filled to capacity with incompressible fluid [4, 5]. And there are many familiar examples of this situation. The inverse problem, in which the final shape is specified and that of the unfilled membrane is sought, is also of interest, with applications to the design of high-altitude scientific balloons [2] and possibly to the construction of automobile airbags [26] and sport hall domes [7, 14].

## References

[1] Abramowitz M. and Stegun I., *Handbook of Mathematical Functions*, Natl. Bureau of Standards, Washington 1964.

[2] Baginski F., *On the Design and Analysus of Inflated Membranes*: *Natural and Pumpkin Shaped Balloons*, SIAM J. Appl. Math. **65** (2005) 838-857.

[3] Byrd P. and Friedman M., *Handbook of Elliptic Integrals for Engineers and Scientists*, 2nd Edn, Springer, New York 1971.

[4] Deakin M., *The Filled Inelastic Membrane*: *A Set of Challenging Problems in the Calculus of Variations*, Bull. Aust. Math. Soc. **80** (2009) 506-509.

[5] Finch S., *Inflating an Inelastic Membrane*, Unpublished notes - 15 August 2013.

[6] Hadzhilazova M. and Mladenov I., *Once More the Mylar Balloon*, C. R. Bulg. Acad. Sci. **61** (2008) 847-856.

[7] Kawaguchi M., *The Shallowest Possible Pneumatic Forms*, Bull. Int. Assoc. Shell Struct. **18** (1977) 3-11.

[8] Krivoshapko S. and Ivanov V., *Encyclopedia of Analytical Surfaces*, Springer, Cham 2015.

[9] Mladenov I., *On the Geometry of the Mylar Balloon*, C. R. Bulg. Acad. Sci. **54** (2001) 39-44.

[10] Mladenov I., *A Case Study of Quantization of Curved Surfaces*: *The Mylar Balloon*, Rend. Circ. Mat. Palermo Ser. II Suppl. **72** (2004) 159–169.

[11] Mladenov I., *New Geometrical Applications of the Elliptic Integrals*: *The Mylar Balloon*, J. Nonlinear Math. Phys. Suppl. **11** (2004) 55–65.

[12] Mladenov I. and Hadzhilazova M., *The Many Faces of Elastica*, Springer, Cham 2017.

[13] Mladenov I. and Oprea J., *The Mylar Balloon Revisited*, Amer. Math. Monthly **110** (2003) 761–784.

[14] Mladenov I. and Oprea J., *On Some Deformations of the Mylar Balloon*, In: Proc. 15th International Workshop on Geometry and Physics in Tenerife 2006, Publ. de la RSME **10** (2007) 308–313.

[15] Mladenov I. and Oprea J., *The Mylar Balloon*: *New Viewpoints and Generalizations*, Geom. Integrability & Quantization **8** (2007) 246-263.

[16] Mladenov I. and Oprea J., *Balloons, Domes and Geometry*, J. Geom. Symmetry Phys. **15** (2009) 53–88.

[17] Mladenov I. and Oprea J., *On the Geometry of the Rotating Liquid Drop*, Math. Comput. Simulat. **127** (2016) 194–202.

[18] Oprea J., *Differential Geometry and Its Applications*, 2$^{\text{nd}}$ Edn, Prentice Hall, Upper Saddle River 2003.

[19] Oprea J., *The Mathematics of Soap Films*: *Explorations with Maple*, Amer. Math. Society, Providence 2000.

[20] Popova E., Hadzhilazova M. and Mladenov I., *On Balloons, Membranes and Surfaces Representing Them*, In: Proc. 35th Spring Conference of UBM, Borovets 2006, pp 201–208.

[21] Paulsen E., *What is the Shape of the Mylar Balloon?*, Amer. Math. Monthly **101** (1994) 953–958.

[22] Pulov V., Hadzhilazova M. and Mladenov I., *The Mylar Balloon*: *An Alternative Description*, Geom. Integrability & Quantization **16** (2015) 255–268.

[23] Toda M. and Pigazzini A., *A Note on the Class of Surfaces with Constant Skew Curvature*, to appear - December 2017.

[24] Wadell H., *Volume, Shape and Roundness of Quartz Particles*, J. Geol. **43** (1935) 250–280.

[25] Whittaker E. and Watson G., *A Course of Modern Analysis*, Cambridge Univ. Press, Cambridge 1927.

[26] Wu C., *The Wrinkled Axisymmetric Air Bags Made of Inextesible Membarne*, J. Appl. Mech. **41** (1974) 963-968.